Arch. Metall. Mater., Vol. 61 (2016), No 2B, p. 957–964

DOI: 10.1515/amm-2016-0163

A. ZIELIŃSKI*#, J. DOBRZAŃSKI*, H. PURZYŃSKA*, G. GOLAŃSKI**

CHANGES IN PROPERTIES AND MICROSTRUCTURE OF HIGH-CHROMIUM 9-12%CR STEELS DUE TO LONG-TERM EXPOSURE AT ELEVATED TEMPERATURE

This paper presents the characteristics of the performance of P91 (X10CrMoVNb9-1), P92 (X10CrWMoVNb9-2) and VM12 (X12CrCoWVNb12-2-2) steels used for condition assessment of the pressure components of boilers with supercritical steam parameters. Studies on the mechanical properties, microstructure tests using scanning and transmission electron microscopy, and X-ray analysis of the phase composition of precipitates were performed for selected steels in the as-received condition and after long-term annealing. These steel characteristics are used for the evaluation of the microstructural changes and mechanical properties of the material of components after long-term service. The result of this study is the database of material characteristics representing the mechanical properties related to the microstructure analysis and it can be used for diagnosis of the components of pressure parts of power boilers.

Keywords: steel P91, P92, VM12, microstructure, mechanical properties, long-term annealing

1. Introduction

The basic requirements placed on all creep-resisting steels are that they should maintain, for a long time, the assumed mechanical properties, high-temperature creep resistance and heat resistance as the elements of safe (reliable) operation within the design working parameters of boiler [1-8].

The new-generation martensitic steels for power engineering were developed by modification of the chemical composition of 9-12%Cr steels used in the power industry so far. These steels are characterised by high mechanical properties; among other things, their creep strength is higher by at least 20-25% than that obtained for steels used so far. The chromium content at the level of 9% in P91 and P92 steels restricts their use up to a temperature of 580-600°C. Also, the carbon content in 9% Cr steels affects the type of existing precipitations and the form of martensite, which is described in great detail, inter alia, in [7,9-11]. Higher chromium content of 12% in VM12 steel is required to ensure the oxidation and gas corrosion resistance during the operation at above 600°C [7].

Long-term impact of elevated temperature during the operation of pressure equipment and systems brings about changes in the microstructure of the material resulting in reduction of mechanical properties. These changes determine the life time of components, which are now designed for 200,000 hours of operation. However, it does not mean that failure-free operation is ensured for such a long time. Therefore, diagnostic works and inspections, and possible repairs are carried out during the boiler's lifetime to ensure safe and failure-free operation of power units.

In safety assessment of the pressure equipment in which new creep-resisting steels were used, it is essential that a number of tests should be carried out to allow the evaluation of their condition and suitability for further operation beyond the design work time under further operation conditions [7,8,12-19].

In cooperation with other research centres (Silesian University of Technology, Czestochowa University of Technology, AGH University of Science and Technology in Cracow) as well as the boiler factories Rafako S.A. and SEFKAO S.A. – the leading manufacturers of boilers, the Institute for Ferrous Metallurgy performs the works on the advance and verification testing of new-generation steels for the power industry [2,7,8,19,21,23].

This study presents the results of investigations on the mechanical properties in the as-received condition as well as the effect of long-term impact of elevated temperature and stress on the change in properties of 9-12%Cr steel.

2. Test sample

The test sample was P91 (X10CrMoVNb9-1), P92 (X10CrWMoVNb9-2) and VM12 (X12CrCoWVNb12-2-2) steels in the as-received condition after heat treatment and after long-term exposure at elevated temperature. The chemical composition of the examined steels is summarised in Table 1.

* INSTITUTE FOR FERROUS METALLURGY, 12-14 K. MIARKI STR., 44-100 GLIWICE, POLAND
** CZĘSTOCHOWA UNIVERSITY OF TECHNOLOGY, INSTITUTE OF MATERIALS ENGINEERING, 19 ARMII KRAJOWEJ AV., 42-200 CZĘSTOCHOWA, POLAND
# Corresponding author: azielinski@imz.pl

TABLE 1

Chemical composition of tested steels

Steel grade	Content of elements [%]												
	–	C	Mn	Si	P	S	Cr	Mo	V	W	Nb	B	N
P91	Mat. testing	0.11	0.41	0.28	0.016	0.004	8.80	0.91	0.22		0.07		0.03
	according to [3]	0.08-0.12	0.30-0.60	0.20-0.50	max 0.02	max 0.01	8.0-9.5	0.85-1.05	0.18-0.25	—	0.06-0.10	—	0.03-0.07
P92	Mat. testing	0.10	0.45	0.17	0.01	0.01	9.26	0.47	0.20	1.95	0.059	0.009	0.04
	according to [3]	0.07-0.13	0.30-0.60	max 0.50	max 0.02	max 0.01	8.5-9.5	0.30-0.60	0.15-0.25	1.5-2.0	0.04-0.09	max 0.006	0.03-0.07
VM12	Mat. testing	0.13	0.22	0.48	0.01	0.01	11.40	0.27	0.22	1.30	0.05	0.003	0.05
	according to [9]	0.11-0.14	0.15-0.45	0.40-0.60	max 0.02	max 0.01	11.0-12.0	0.20-0.40	0.20-0.30	1.30-1.70	0.03-0.08	0.003-0.006	0.03-0.07

3. Scope of tests

The tests performed on selected grades of P91, P92 and VM12 steels in both the as-received condition and after long-term annealing for up to 30,000 h at 600 and 650°C included the following:

- static tensile test at room and elevated temperature using Zwick tensile testing machine with max load of 200 kN.
- hardness measurement by Vickers method with Future – Tech FM – 7 hardness testing machine using the indenter load of 10 kG,
- impact test on standard V-notched test samples,
- microstructure investigations with Inspect F scanning electron microscope (SEM) on conventionally prepared metallographic microsections etched with ferric chloride,
- analysis of precipitation processes by X-ray analysis of carbide isolates with Philips diffractometer.

4. Test results

Mechanical properties

In their as-received condition, the tested steels are characterised by high mechanical properties (Table 2). P91 steel in as-received state exhibits by approx. 10% higher tensile strength and yield point at room temperature, while its yield point at a temperature similar to the expected working temperature is by approx. 20% higher than that required for this steel [3]. Also, the impact strength of P91 steel exceeds the requirements for the material in the as-received condition to a significant extent and is approx. 10 times as high compared with the required minimum of 27J.

P91 and VM12 steels in the as-received condition are characterised by approx. 20% higher tensile strength and yield point at room temperature and by approx. 10% higher yield point at 550°C in relation to the minimum requirements. Impact strength of P92 and VM12 is 6 and 3 times as high as the required minimum for these steel grades, respectively. Such a significant difference in impact strength of VM12 steel compared to P91 and P92 steels is the effect of high carbon content (lower by only 0.01% than the required maximum allowable content of this element), which results in increase in the amount of $M_{23}C_6$ carbides and martensite laths precipitated at the prior austenite grain boundaries. It has an adverse impact on the ductility of the tested steel. Lower impact strength of VM12 steel in the as-received condition compared to other martensitic steels is also affected by the existence of delta ferrite observed in the microstructure. For the tested steels, only the elongation value is merely slightly higher than the required minimum [3,12].

TABLE 2

Mechanical properties of tested steels in the as-received condition

Steel grade	TS, [MPa]	YS, [MPa]	YS^{550}, [MPa]	El., [%]	RA, [%]	KV, [J]	HV10
P91 [3]	620÷850	min. 450	min. 287	min. 19	—	min. 27	—
Tested P91 steel	679	509	372	25	66	255	232
P92 [3]	620÷850	min. 440	min. 300	min. 19	—	min. 27	—
Tested P92 steel	735	562	340	19	63	161	225
VM12 [9]	620÷850	min. 450	min. 300	min. 19	—	min. 27	—
Tested VM12 steel	750	571	338	23	64	78	259

The effects of long-term annealing at 600 and 650°C on mechanical properties of P91, P92 and VM12 steels are shown in Tables 3-5. Long-term annealing at 600 and 650°C and after soaking time of up to 30,000 hours had only a slight impact on the reduction in strength properties, i.e. yield point and tensile strength, both at room temperature and elevated temperature similar to the expected working temperature.

TABLE 3

Comparison of the results of mechanical properties investigations of P91 steel after long-term annealing

	As-received condition	**Annealing 1000h/600°C**	**Annealing 5000h/600°C**	**Annealing 10000h/600°C**	**Annealing 30000h/600°C**
TS, [MPa]	679	677	689	671	669
YS, [MPa]	509	508	518	500	498
El., [%]	25	25	24	22	21
YS^{550}, [MPa]	360	329	349	336	328
HV10	232	218	219	210	200
Impact energy [KV], J	201	193	147	131	121
	As-received condition	**Annealing 1000h/650°C**	**Annealing 5000h/650°C**	**Annealing 10000h/650°C**	**Annealing 30000h/650°C**
TS, [MPa]	679	675	670	665	668
YS, [MPa]	509	502	495	496	501
El., [%]	25	24	24	23	20
YS^{550}, [MPa]	360	348	354	338	320
HV10	232	224	215	213	198
Impact energy KV, [J]	201	195	165	172	153

The insignificant reduction in strength properties of the tested steels after 30,000 h annealing, not exceeding 10%, shows a very slow matrix recovery and polygonisation process and the disappearance of tempered martensite lath microstructure, as these steels are characterised by metastable tempered martensite lath microstructure with high-density dislocation. Further temperature and time impact may result in gradual disappearance of lath microstructure by dislocation movement until the increase in amount and size of precipitates and the reduction in dislocation density occur. The consequence will be gradual reduction in strength properties.

TABLE 4

Comparison of the results of mechanical properties investigations of P92 steel after long-term annealing

	As-received condition	**Annealing 1000h/600°C**	**Annealing 5000h/600°C**	**Annealing 10000h/600°C**	**Annealing 30000h/600°C**
TS, [MPa]	735	736	724	725	695
YS, [MPa]	562	536	525	520	515
El., [%]	18	23	24	22	20
YS^{550}, [MPa]	340	345	335	332	320
HV10	225	220	214	210	207
Impact energy [KV], J	161	59	47	51	44
	As-received condition	**Annealing 1000h/650°C**	**Annealing 5000h/650°C**	**Annealing 10000h/650°C**	**Annealing 30000h/650°C**
TS, [MPa]	735	728	720	718	692
YS, [MPa]	562	534	515	519	508
El., [%]	18	21	22	20	18
YS^{550}, [MPa]	340	348	328	336	312
HV10	225	222	207	213	203
Impact energy KV, [J]	161	90	49	52	38

TABLE 5

Comparison of the results of mechanical properties investigations of VM12 steel after long-term annealing

	As-received condition	**Annealing 1000h/600°C**	**Annealing 5000h/600°C**	**Annealing 10000h/600°C**	**Annealing 30000h/600°C**
TS, [MPa]	750	706	702	724	723
YS, [MPa]	571	514	512	540	533
El., [%]	23	25	25	23	23
YS^{550}, [MPa]	338	332	338	329	315
HV10	259	244	235	239	218
Impact energy [KV], J	78	49	43	41	38

	As-received condition	Annealing 1000h/650°C	Annealing 5000h/650°C	Annealing 10000h/650°C	Annealing 30000h/650°C
TS, [MPa]	750	736	735	721	706
YS, [MPa]	571	536	536	519	495
El., [%]	23	25	20	22	19
YS^{550}, [MPa]	338	349	352	328	298
HV10	259	223	236	229	207
Impact energy KV, [J]	78	47	39	30	29

The similar nature of small changes with the extension of the annealing time was observed in hardness of the tested steels. For these steels, the continuous but insignificant reduction in hardness HV10 was observed. It was 15, 10 and 15% for P91, P92 and VM12 steels, respectively. This trend is certainly related to the disappearance of fine-dispersion MX precipitates, and thus to the decrease in precipitation hardening.

A slight reduction in strength properties and hardness of the tested steels when annealing for up to 30,000 hours at 600 and 650°C was accompanied by the significant reduction in impact strength.

The highest loss of the impact energy compared to the as-received condition (160J) was found in P92 steel after annealing for 30000 h, reaching the level of 50J. However, it is significantly higher than the required minimum of 27J. Similarly as P92 steel, VM12 is also characterised by significant reduction in the impact energy depending on the annealing time, which fell from 78J in the as-received condition to approx. 38J after 30000 h annealing at 600°C and to 29J after annealing at 650°C, which corresponds to the minimum requirement of 27J. Out of the tested steels, the highest impact energy level after long-term annealing was revealed in the case of P91 steel. The impact energy of this steel after 30000 h annealing at 600 and 650°C is 121 and 153J, respectively.

The decrease in impact strength as early as after 1000 h annealing in 9-12%Cr steels is connected most probably with the increase in subgrain width and the dynamics of the increase in amount and size of $M_{23}C_6$ carbide precipitations, as well as the Laves phase precipitation at the prior austenite grain boundaries. It is conducive to the reduction in their decohesion and results in the increase of tendency to cleavage fracture [19,20].

Microstructure

The long-term high-temperature impact on the microstructure of the tested steels is controlled by thermally activated processes. These processes accelerate as the temperature rises, at the same time reducing the set of functional properties of both the material and the component made of it. The steel microstructure is subject to changes consisting in disappearance of the output structural components and precipitation processes the course of which is the competing dissolution and secondary precipitation processes. The evaluation of structural changes with regard to the level of functional properties is one of the elements of materials characteristics of steels designed for service under creep conditions.

The investigations of microstructure were carried out for the tested steels in the as-received condition and after long-term annealing at 600 and 650°C. The microstructure images of the P91, P92 and VM12 steels in the as-received condition and after 30,000 h annealing at 600 and 650°C observed under scanning and transmission electron microscope are shown in Fig. 1-3.

The P91 steel in the as-received condition is characterised by tempered martensite microstructure with fine-dispersion MX precipitates, mainly of vanadium, and vanadium and niobium-rich precipitations and also $M_{23}C_6$ carbides. The precipitates occur both at the grain boundaries and inside ferrite grains (Fig. 1a,b). The precipitation hardening in this steel is the result of existence of numerous fine carbonitride precipitates, which have also significant impact on the improvement in creep strength. The $M_{23}C_6$ carbides existing in steel stabilise the lath martensite microstructure.

The visible changes in the microstructure image of P91 steel after annealing for 30,000h at 600°C, compared to the as-received condition, caused by long-term temperature impact, are shown in Fig. 1c. The increase in the size of precipitates was found after this time of annealing. The increase in the size of precipitates observed in this paper is also presented in [4,17]. As expected, their size was bigger after long-term annealing at 650ºC (Fig. 1d). Also, the effects of progressing martensite tempering processes could be observed. Bigger and more densely arranged $M_{23}C_6$ carbide precipitates at the prior austenite grain boundaries and inside ferrite grains were revealed.

In the as-received condition, the P92 steel is characterised by the microstructure with predominating content of tempered lath martensite with high-density dislocation and polygonised substructure of ferrite grains (Fig. 2a,b), typical of this group of steels [17]. The identification of precipitates revealed the existence of the following types of precipitates in the tested steel in the as-received condition: MX and $M_{23}C_6$ [29]. MX precipitates were observed inside martensite laths, at dislocations and at the subgrain boundaries. On the other hand, $M_{23}C_6$ carbides were mainly revealed at the prior austenite grain boundaries and at the martensite lath boundaries. The results of the identification performed by the selective electron diffraction method with TEM were confirmed by the X-ray phase analysis of isolated precipitation [29] (Table 6).

The extension of the duration of annealing up to 30,000 h resulted in local or partial disappearance of the lath microstructure of tempered martensite areas at test temperature of 600°C (Fig. 2c). For annealing at 650°C, further progressing decomposition of lath martensite microstructure was observed (Fig. 2d). This microstructure was characterised by still preserved martensitic microstructure with numerous different size precipitates at the prior

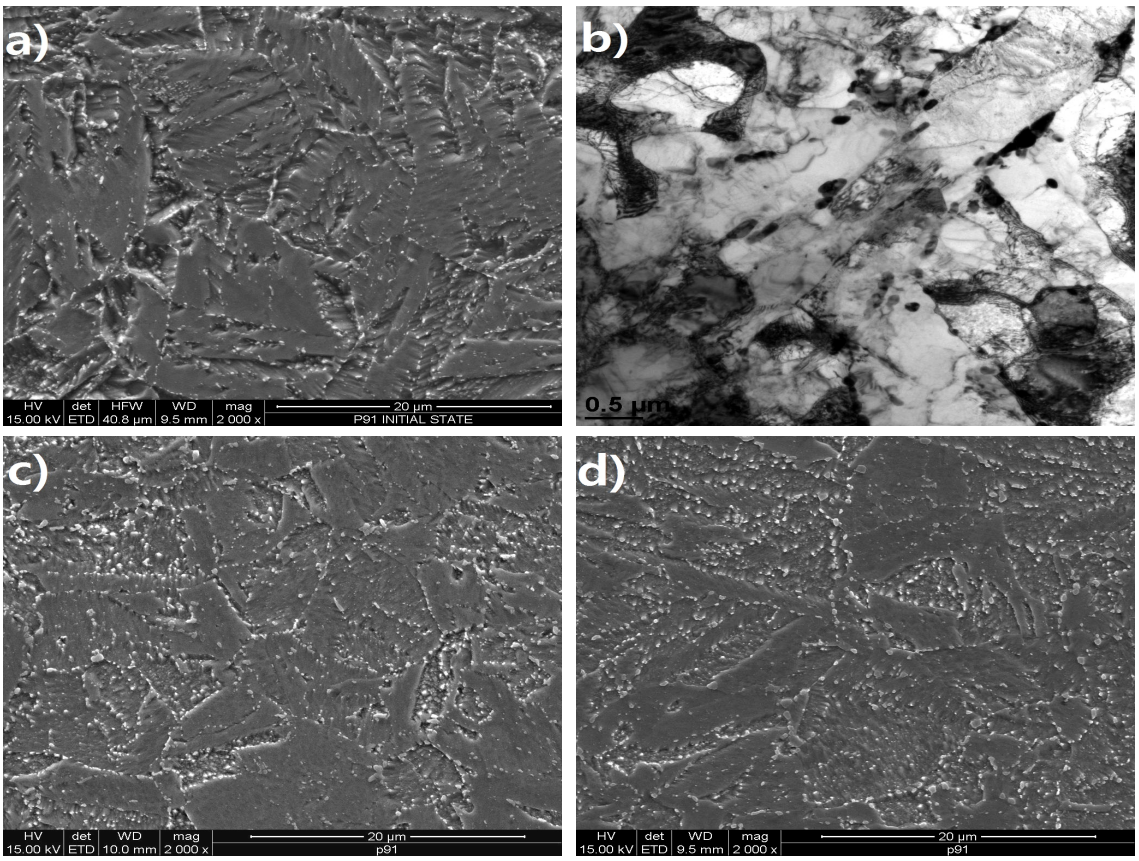

Fig. 1. Microstructure images of P91 steel a) in the as-received condition SEM, b) in the as-received condition TEM, c) after 30,000h/600°C annealing, d) after 30,000h/650°C annealing

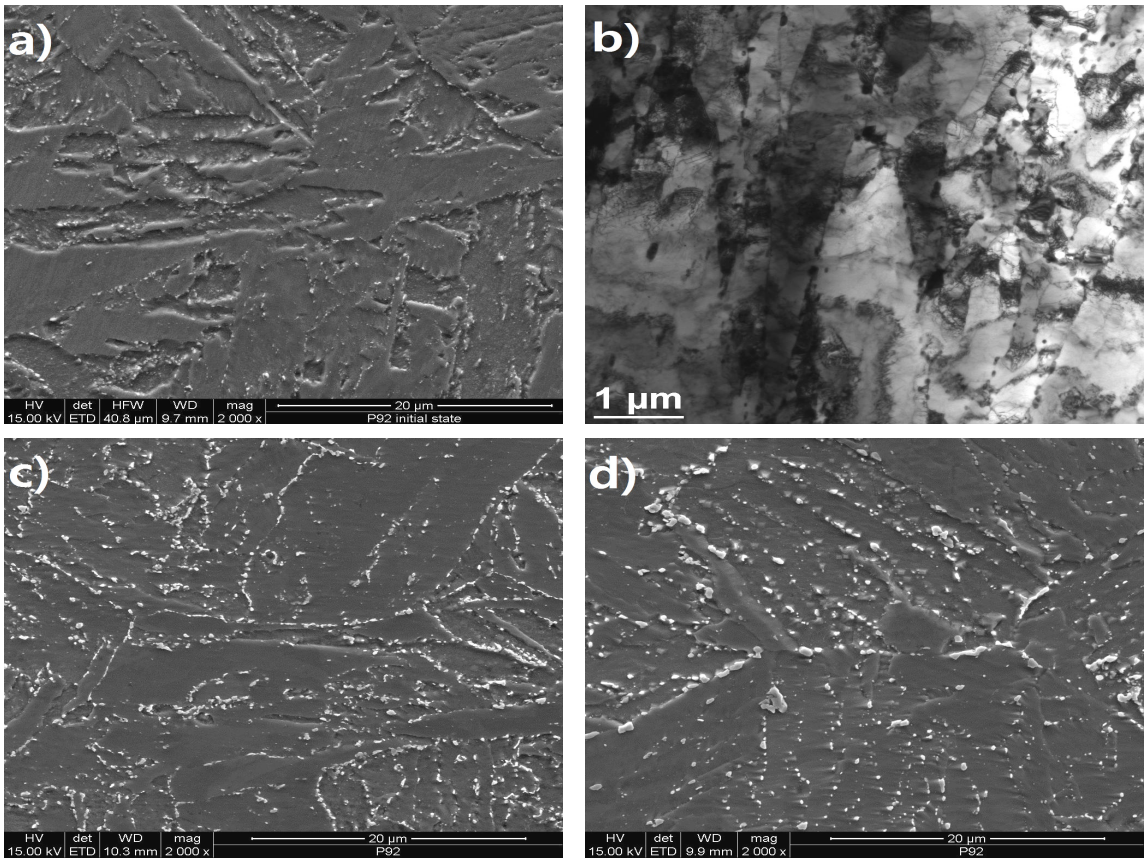

Fig. 2. Microstructure images of P92 steel a) in the as-received SEM, b) in the as-received TEM, c) after 30,000h/600°C annealing, d) after 30,000h/650°C annealing

austenite grain and martensite lath boundaries. As compared to the microstructure observed for the same duration of annealing and temperature of 600°C (Fig. 2c), the difference in the size of existing precipitates is noticeable (Fig. 2d). These results are also presented in [5]. In both the analysed microstructures, areas were observed where the amount of precipitates at the grain boundaries was so high that they formed the continuous network of precipitates.

In the as-received condition, the VM12 steel is characterised by high-tempered lath martensite microstructure with numerous precipitates (Fig. 3a,b). As shown by the investigations [29], $M_{23}C_6$ carbides and MX precipitates were revealed in the VM12 steel in the as-received condition. $M_{23}C_6$ carbides (carboborides) mainly occurred at the prior austenite grain boundaries and at the martensite subgrain/lath boundaries. MX nitrides (carbonitrides) were mainly precipitated inside subgrains and at the subgrain boundaries. $M_{23}C_6$ carbides stabilise the subgrain microstructure of martensitic steel, while fine-dispersion MX precipitates are the effective barrier for dislocation movement, thus ensuring high creep strength. The existence of delta ferrite was also revealed in the microstructure of the tested steel.

Figures 3c and 3d present the example microstructures of VM12 steel after 30,000 h annealing at 600 and 650°C. The observations of the microstructure of VM12 steel annealed at 600°C for 30,000h revealed the noticeable increase in the size of precipitates at the prior austenite grain boundaries, at the martensite lath boundaries and inside grains. The insignificant disappearance of tempered martensite microstructure was also observed. After annealing at 650°C for 30,000 h, there was an significant increase in the size of precipitates at the prior austenite grain boundaries, at the martensite lath boundaries and inside grains compared to, not only the as-received condition of VM12 steel, but also in relation to the same time of annealing at 600°C [7]. A partial disappearance of the tempered lath martensite microstructure is also visible (Fig. 3d).

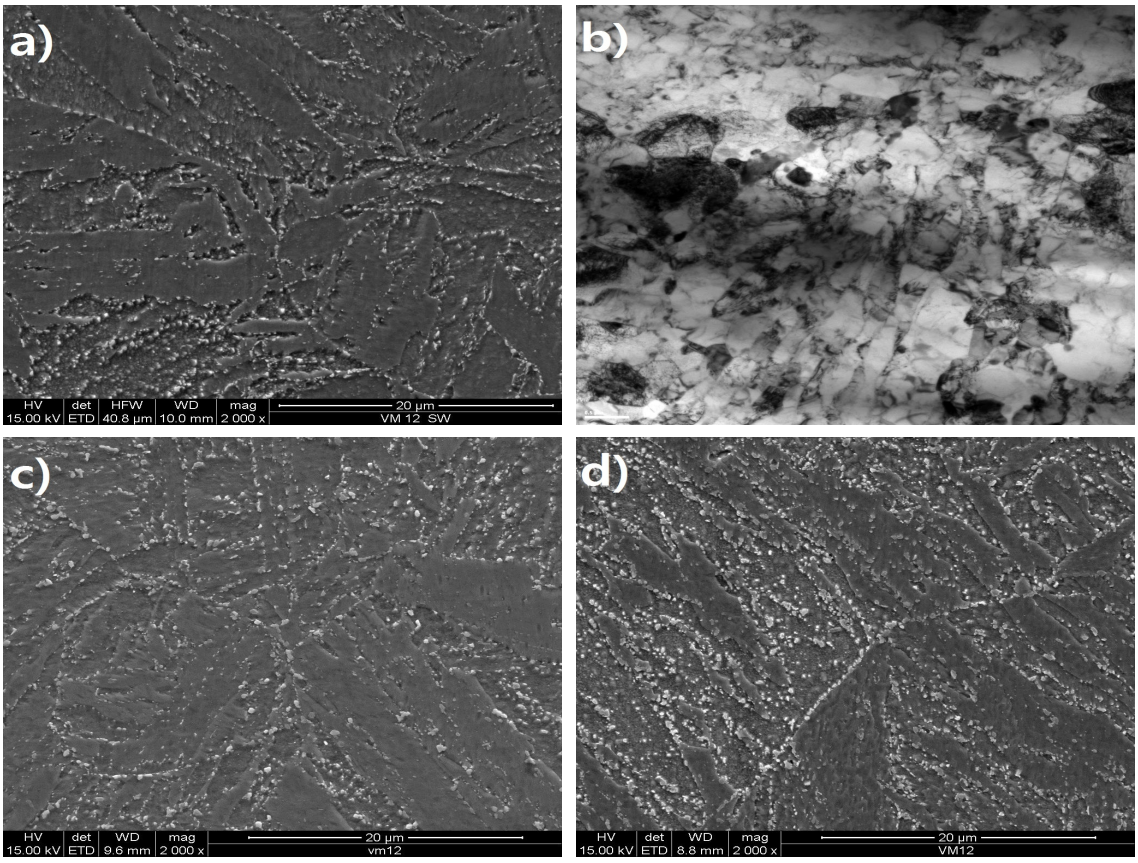

Fig. 3. Microstructure images of MV12 steel a) in the as-received SEM, b) in the as-received TEM, c) after 30,000h/600°C annealing, d) after 30,000h/650°C annealing

Impact of long-term annealing on the phase composition of precipitates

During the operation of 9-12% Cr steels at elevated temperature, there are changes occurring in the microstructure (disappearance of the martensite lath microstructure), as well as changes in the amount, size, shape and type of precipitated carbides, depending on chemical composition and initial microstructure of the steel. Thus, the occurrence of individual types of precipitates is related to the degree of microstructure degradation. The identification of the existing precipitates and the assessment of their shares in the tested steels were carried out using the transmission electron microscopy and by means of the X-ray phase analysis of isolated precipitation deposits [2].

The X-ray diffractograms of isolates were obtained on Philips PW 1140 diffractometer, using cobalt radiation with

graphite monochromator on the diffracted beam side. The qualitative analysis of carbide precipitates was carried out based on standard roentgenographic data from the International Centre for Diffraction Data PDF-4 database. The phase composition analysis of the precipitates was carried out for the tested steels in the as-received condition and after long-term annealing at 600 and 650°C. The phase composition of the precipitates is summarised in Table 6.

TABLE 6

Phase composition of precipitates in P91, P92 and VM12 steels in the as-received condition and after long-term annealing up to 30,000 hours

Material condition / Steel grade	**Phase components**	**Material condition**	**Phase components**
as-received condition P91	$M_{23}C_6$ containing mainly Cr – main phase Nb(C, N)	—	—
annealing 10,000h/600°C P91	$M_{23}C_6$ containing mainly Cr Small amounts of Fe_2Mo V(C,N)	annealing 10,000h/650°C P91	$M_{23}C_6$ containing mainly Cr Fe_2Mo M_6C containing mainly Fe, Mo Nb(C, N) V(C,N)
annealing 30,000h/600°C P91	$M_{23}C_6$ containing mainly Cr Small amounts of Fe_2Mo M_6C containing mainly Fe, Mo V(C,N)	annealing 30,000h/650°C P91	$M_{23}C_6$ containing mainly Cr Fe_2Mo M_6C containing mainly Fe, Mo Nb(C, N) V(C,N)
as-received condition P92	$M_{23}C_6$ containing mainly Cr – main phase Nb(C, N) V(C,N)	—	—
annealing 10,000h/600°C P92	$M_{23}C_6$ containing mainly Cr Small amounts of Fe_2Mo M_6C containing mainly Fe, Mo V(C,N)	annealing 10,000h/650°C P92	$M_{23}C_6$ containing mainly Cr $Fe_2(Mo,W)$, V(C,N) M_6C containing mainly Fe, Mo, Ni
annealing 30,000h/600°C P92	$M_{23}C_6$ containing mainly Cr $Fe_2(Mo,W)$ M_6C containing mainly Fe, Mo V(C,N)	annealing 30,000h/650°C P92	$M_{23}C_6$ containing mainly Cr $Fe_2(Mo,W)$, V(C,N) M_6C containing mainly Fe, Mo, Ni
as-received condition VM12	$M_{23}C_6$ – main phase MN	—	—
annealing 10,000h/600°C VM12	Main phase $M_{23}C_6$ (Fe_2Mo) – small amount, NbCrN – medium	annealing 10,000h/650°C VM12	Main phase $M_{23}C_6$ medium – Laves phase Fe_2Mo NbCrN
annealing 30,000h/600°C VM12	Main phase $M_{23}C_6$ (Fe_2Mo) – small amount, NbCrN – medium	annealing 30,000h/650°C VM12	Main phase $M_{23}C_6$ medium – Laves phase Fe_2Mo NbCrN

The existence of $M_{23}C_6$ carbides, niobium carbonitrides and MC carbides containing vanadium in P91 and P92 steels in the as-received condition was confirmed by the rentgenographic examinations. The results of this analyses are consistent with the literature data [17].

The annealing of P91 steel at both 600 and 650°C for up to 30,000 hours results in the increase in the amount of $M_{23}C_6$ precipitates, precipitation of molybdenum-rich M_6C carbides and Fe_2Mo Laves phase.

After annealing at 600°C for 10,000 hours, the precipitations of Fe_2Mo Laves phase were observed in the P92 steel, while after annealing at 650°C for 10,000 h the precipitations of Fe_2W tungsten-rich Laves phase. The annealing at 600 and 650°C for 30,000 h results in the increase in the size and amount of precipitates, mainly of molybdenum and tungsten-rich Laves phase.

The phase composition analysis of precipitates in the VM12 steel after annealing at 600 and 650°C revealed the existence of Laves phase and probable transformation of MN precipitates into more stable Z phase, which results in reduced creep strength [7,31,32]. Each large precipitation of Z phase occurs at the expense of ca. 1500 fine-dispersive MX precipitates [31].

The impact of the Laves phase on the performance of the tested steels is explicitly negative. The precipitation and growth of the Laves phase makes the matrix deplete of substitution elements (chromium, molybdenum, tungsten) as a result of their diffusion from the matrix into this phase, which results in acceleration of the matrix recovery and polygonisation processes. The Laves phase precipitates mainly at the prior austenite grain boundaries, nearby $M_{23}C_6$ carbides. At the same time, the depletion of alloying elements in the matrix, which are also the components of $M_{23}C_6$ carbides, results in slowing down the coagulation of these carbides. In addition, the Laves phase that precipitates at the boundaries has an adverse impact on ductility. According to the tests [30], the Laves phase precipitations with average diameter higher than 130 nm contribute to the change in the cracking mechanism of high-temperature creep resisting

steel from ductile to brittle (transcrystalline cleavable fracture) and are the main reason for the sudden reduction in creep strength of 9% Cr steels.

5. Summary

The completed investigations of mechanical properties and microstructure of P91, P92 and VM12 steels in the as-received condition and after 30,000 h annealing at 600 and 650°C allowed the following conclusions to be drawn:

1. The obtained values of mechanical properties after long-term annealing only slightly deviate from those in the as-received condition, and after 30,000 h exposure at elevated temperature (Table 3, 4, 5), they meet the requirements for the tested steels in the as-received condition (Table 2). The highest decrease in their values is observed for the impact energy of the tested steels out of which VM12 showed the highest impact energy loss from 78J for the as-received condition to 29J after annealing at 650°C for 30,000 h.
2. As a result of increasing the time of exposure at elevated temperature, the microstructure of the tested steels is subject to continuous degradation, which manifests itself in the increased amount and size of precipitates at the prior austenite grain boundaries and the martensite lath boundaries [4,5,7,17]. As expected, the highest microstructure degradation was observed for the tested steels after 30,000 h annealing at 650°C (Fig. 1d, 2d, 3d). The highest degree of degradation is confirmed by phase composition of the precipitates (Table 6). Following the longest time of annealing at 650°C, i.e. 30,000 h, the main phase of precipitates in P91, P92 and VM12 steels is $M_{23}C_6$ carbides.
3. The result of this study is the database of material characteristics representing the mechanical properties related to the microstructure analysis (degree of degradation and precipitation processes) and it is used for diagnosis of the components of pressure parts of power boilers.

REFERENCES

[1] J. Dobrzański, Materials science interpretation of the life of steels for power plants, Open Access Library 3, (2011).

[2] A. Zieliński, M. Miczka, M. Sroka, Mater. Sci. Tech-Lond. (2016), DOI: 10.1080/02670836.2016.1150242, (in press).

[3] PN-EN 10216-2, January 2009, Seamless steel tubes for pressure purposes. Technical delivery conditions. Part 2: Non-alloy and alloy steel tubes with specified elevated temperature properties.

[4] A. Zieliński, G. Golański, M. Sroka, J. Dobrzański, Mater. Sci. Tech. (2015), DOI: 1743284715Y-0000000137, (in press).

[5] A. Zieliński, G. Golański, M. Sroka, T. Tański, (2015), Mater. High Temp. 1878641315Y-0000000015, (in press).

[6] G. Golański, J. Kępa, Mater. Sc. **32**, 6, 917-922, (2011).

[7] A. Zieliński, G. Golański, M. Sroka, P. Skupień, Mater. High Temp. **33**, 2, 154-163 (2016).

[8] J. Dobrzański, A. Zieliński, M. Sroka, J. of Achiev. Mater. Manufact. Eng. **34**, 1, 7-14, (2009).

[9] V. Sklenicka, K. Kucharova, M. Svoboda, L. Kloc, J. Bursik, A. Kroupa, Mater. Charact. **51**, 35-48, (2003)

[10] J. Hald, Int. J. Pres. Ves. Pip. **85**, 30-37, (2008).

[11] F. Abe, T. Horiuchi, M. Taneike, K. Sawadad, Mat. Sci. Eng. A-Struct. **378**, 299-303, (2004).

[12] J. Gabrel, W. Bendick, J. C. Vaillant, B. Vandenberghe, B. Lefebvre, Advances in Materials Technology for Fossil Power Plants. **919**, (2004).

[13] Data Package for NF616 Ferritic steel (Cr-0,5Mo-1,8W-Nb-V), Nippon Steel Corporation, January (1993).

[14] F. Abe, M. T. Horiuchi, M. Taneike, K. Sawada, Mat. Sci. Eng. A **378**, 299 (2004).

[15] H. Semba, F. Abe, Materials for Advanced Power Engineering, Forschungszentrum Jülich 1041-1052, (2006).

[16] V. Sklenicka, K. Kucharova, M. Svoboda, L. Kloc, J. Kudrman, Materials for Advanced Power Engineering 2006, Forschungszentrum Jülich, 1127-1136, (2006).

[17] A. Zielińska-Lipiec, The Analysis of Microstructural Stability of Modified Martensitic Deformation, (2005), Poland.

[18] A. Zielinska-Lipiec, T. Kozieł, A. Czyrska-Filemonowicz, J. Achiev. Mater. Manufact. Eng. **43**(1), 200-204 (2010).

[19] G. Golański, The Czestochowa University of Technology Publishing House. Czestochowa 49-51 (2012)

[20] R.M. Horn, R.O. Ritchie, Metall. Trans. A 9A, 1039-1053 (1978).

[21] J. Dobrzański, A. Zieliński, A. Maciosowski, IMŻ Report No. S0-0438/2003, (unpublished), (2003).

[22] B.J. Kim, B.S. Lim, Proceedings of the 13th International Conference on Experimental Mechanics, Alexandroupolis, Greece, July 1-6, 269-270, (2007).

[23] A. Zieliński, J. Dobrzański, H. Krztoń, J. Achiev. Mater. Manufact. Eng. **25**, 1, 33-36, (2007).

[24] NIMS Creep date sheet No43, Japan (1996).

[25] C. Chovet, E. Galand, G. Ehrhart, E. Baune, B. Leduey, Proceedings of the II W. International Conference, 10-11 July , Graz Austria, 443-448, (2008).

[26] G. Golański, A. Zieliński, Metallurgy – Metallurgical Engineering News No. **3**, 228-233, (2011).

[27] R. M. Horn, R.O. Ritchie, Metall. Trans. A, 9A, 1039-1053, (1978).

[28] N. Bandyopadhyay, Jr C. J.McMahon, Metall. Trans. A, 14A, 1313 – 1325, (1983).

[29] J. Dobrzański, A. Zieliński, H. Paszkowska, Development Project No. 15 0060 10 realised at the Institute for Ferrous Metallurgy, (unpublished), (2013)

[30] S. Lee, H.G. Armaki, K. Maruyama, T. Muraki, H. Asahi, Mater. Sc. Eng. A, **428**, 270-275, (2006).

[31] H.K. Danielsen, J. Hald, VGB PowerTech. **5**, 68-73, (2009).

[32] R.O. Kaibyshev, V.N. Skorobogatykh, I. A. Shchenkova, Metal Sc. and Heat Treatment **52**, 90-99, (2010).